Design and Analysis of Iris-Coupled and Dielectric-Loaded 1/8-Cut TE_{01}-Mode Microwave Bandpass Filters

Smain Amari, *Member, IEEE*, Jens Bornemann, *Senior Member, IEEE*, Alexandre Laisné, and Rüdiger Vahldieck, *Fellow, IEEE*

***Abstract*—The design and analysis of iris-coupled and dielectric-loaded 1/8-cut TE_{01}-mode filters is performed using globalized local solutions of Maxwell's equations as basis functions. It is found that this set of basis functions outperforms other edge-conditioned basis functions. To reduce the size of the filter and increase the Q factor of the resonators, dielectric rings with high dielectric constant are employed in the same design technique. The dimensions of the resonators are determined to accurately take into account the effect of coupling on their resonant frequencies, thereby reducing the need of tuning. Numerical results are compared with those obtained from the finite-element method (HP HFSS) and the mode-matching technique. Good agreement is demonstrated.**

***Index Terms*—Bandpass filters, dielectric resonator filters, integral equations, waveguide filters.**

I. Introduction

MICROWAVE filters, which have been the subject of intensive research efforts over the past decades, permeate modern communication systems whose proper performance is achieved only through accurately designed components. Furthermore, the increasing demand on frequency bandwidth requires filters with extremely narrow bandwidths whose precise design is even more demanding. Waveguide resonators have been, and are still, used as building blocks in microwave filter implementation. Judicious coupling between the different resonators is essential to the proper performance of the filter, especially for narrow-band filters where the weak coupling must be determined with high accuracy to guarantee the proper performance of the designed filter.

The mode-matching technique (MMT), e.g., [1], has been used extensively in the analysis and design of waveguide components such as filters. Unfortunately, the MMT exhibits slow convergence for narrow-band systems due to its failure to account for the singular nature of the electromagnetic field at sharp metallic edges. An alternative formulation that provides a simple mechanism including *a priori* information such as the edge conditions was recently developed [2]. It consists of deriving a set of coupled integral equations for the aperture fields at all discontinuities simultaneously. The coupled-integral-equation technique (CIET) allows accurate and fast design and analysis of narrow-band rectangular waveguide structures [3].

In this paper, we improve the efficiency of the CIET by using local solutions of Maxwell's equations, which are properly globalized to satisfy other boundary conditions, in the analysis and design of TE_{01}-mode iris-coupled bandpass filters. To improve the stopband response of the filter, 1/8-cut circular waveguides instead of full cylindrical waveguides are used to suppress unwanted propagating modes. Although the reduced volume of the resonators lowers the Q factor of the resonators because of metallic losses in the conducting walls, the addition of high-Q dielectric rings can be used to compensate for such a reduction while allowing further size shrinking. Bandpass microwave filters using dielectric resonators in cutoff waveguides have been investigated by many researchers, e.g., [4]–[8]. The design of the filter usually starts from determining the size of the dielectric resonator such that its resonant frequency is equal to the center frequency of the bandpass filter. The coupling coefficients between the resonators are then determined from two separate analyses of the resonant frequencies of the two coupled resonators with an electric and then a magnetic wall placed between them [6]–[8]. However, such an approach neglects the shift in the resonant frequency due to the loading caused by the coupling; tuning mechanisms must then be used to compensate for the occurred shifts.

It is also possible to use the standard design technique of waveguide resonator filters to design the class of iris-coupled and dielectric-loaded resonators considered in this paper. This approach was used in designing E-plane dielectric waveguide filters [9] as well as TE_{01}-mode dielectric-loaded rectangular filters [10]. Within this framework, it is possible to determine accurately the coupling between the resonators while taking into account its effect on the resonant frequencies of the resonators. In fact, it is not even necessary to determine the resonant frequency of the resonators. The designed filters are then analyzed using HFSS to validate the results obtained from the CIET.

II. Synthesis and Design of Iris-Coupled 1/8-Cut TE_{01}-Mode Filters

The synthesis of the class of filters under consideration follows the standard inverter approach [11], [12]. Since the method

Manuscript received August 31, 1999.

S. Amari and J. Bornemann are with the Department of Electrical and Computer Engineering, University of Victoria, Victoria, BC, Canada V8W 3P6.

A. Laisné was with the Department of Electrical and Computer Engineering, University of Victoria, Victoria, BC, Canada V8W 3P6. He is now with the National Institute of Applied Sciences (INSA), Rennes 35043, France.

R. Vahldieck is with the Swiss Federal Institute of Technology, Zürich 8092, Switzerland.

Publisher Item Identifier S 0018-9480(01)01675-1.

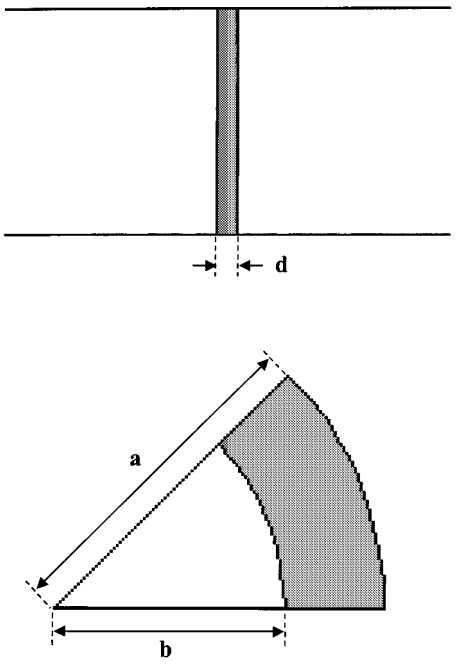

Fig. 1. (top) Side view and (bottom) cross section of a coupling iris for 1/8-cut TE_{01}-mode bandpass filters.

is well documented, it is not discussed here. Suffice it to say that the scattering parameters of the dominant mode at the iris are iteratively determined from the following equations:

$$X_s = \mathrm{Im}\,\frac{1+S_{11}-S_{21}}{1-S_{11}+S_{21}} \tag{1}$$

$$X_p = \mathrm{Im}\,\frac{2S_{21}}{(1-S_{11})^2-S_{21}^2} \tag{2}$$

$$\Phi = -\tan^{-1}\left(\frac{2(X_p+X_s)}{1-X_s^2-2X_sX_p}\right) \tag{3}$$

$$K = \left|\tan\left(\frac{\Phi}{2}+\tan^{-1}(X_s)\right)\right|. \tag{4}$$

Here, S_{11} and S_{21} are the scattering parameters of the TE_{01} mode at the iris computed at the center frequency of the passband.

The target values of the inverters K are determined from the low-pass prototype [12]. Once the dimensions of the coupling sections are determined, the length of the resonators connected to it are adjusted by the phase term

$$l_i = \frac{1}{\beta}\left(\pi+\frac{\Phi_i+\Phi_{i+1}}{2}\right) \tag{5}$$

where β is the propagation constant of the dominant mode at the center frequency of the passband. The structure used to implement a typical coupling section is presented in Fig. 1. It consists of 1/8-cut circular waveguide of radius a, and a circular iris of thickness d and inner radius b. We assume that all metallic walls are lossless and that only the TE_{01} mode is incident on the iris. Due to the symmetry of the structure, only TE_{0n} modes are excited at the discontinuity. The determination of the radius of the empty waveguide can be done such as to minimize the effect of higher order evanescent modes in order for this design technique to work as expected. Although it is possible to include corrections in the design, especially for broadband designs [13], we choose the radius of the empty waveguide such that the damping of the first evanescent mode over a guided half-wavelength of the dominant propagating mode is less than $e^{(-5)}$ at the center frequency; this condition is sufficient to determine the radius of the waveguide.

To determine the radius of the coupling irises, assuming that their thickness is known, their scattering properties must be iteratively and accurately determined at the center frequency of the filter until (1)–(4) are satisfied. An accurate design can be achieved by using the CIET with appropriate basis functions as shown below.

Since the derivation of the integral equations for the aperture fields follows the presentation in [2], we only give the final equations for those interested in applying the approach in design problems.

Let us assume that the exact distribution of E_ϕ at the two discontinuities of Fig. 1 are given by two unknown functions $X_1(\rho)$ and $X_2(\rho)$. These can be determined from the following two coupled integral equations:

$$\sum_{m=1}^{\infty} g_m^{\mathrm{II}} Y_m^{\mathrm{II}} \frac{\tilde{X}_1^{\mathrm{II}}(m)\cos\left[k_{zm}^{\mathrm{II}}d\right]-\tilde{X}_2^{\mathrm{II}}(m)}{j\sin\left[k_{zm}^{\mathrm{II}}d\right]} J_1\left(\frac{x_{m1}}{b}\rho\right) + \sum_{m=1}^{\infty} Y_m^{\mathrm{I}}\tilde{X}_1^{\mathrm{I}}(m) g_m^{\mathrm{I}} J_1\left(\frac{x_{m1}}{a}\rho\right) = 2Y_1^{\mathrm{I}} g_1^{\mathrm{I}} J_1\left(\frac{x_{11}}{a}\rho\right) \tag{6}$$

and

$$\sum_{m=1}^{\infty} g_m^{\mathrm{II}} Y_m^{\mathrm{II}} \frac{\tilde{X}_2^{\mathrm{II}}(m)\cos\left[k_{zm}^{\mathrm{II}}d\right]-\tilde{X}_1^{\mathrm{II}}(m)}{j\sin\left[k_{zm}^{\mathrm{II}}d\right]} J_1\left(\frac{x_{m1}}{b}\rho\right) + \sum_{m=1}^{\infty} Y_m^{\mathrm{I}}\tilde{X}_2^{\mathrm{I}}(m) g_m^{\mathrm{I}} J_1\left(\frac{x_{m1}}{a}\rho\right) = 0. \tag{7}$$

Here, J_1 is the Bessel function of the first kind of order one and x_{m1} is its root of order m

$$\begin{aligned} k_{zm}^{\mathrm{I}} &= \sqrt{k_0^2-\left(\frac{x_{m1}}{a}\right)^2} \\ k_{zm}^{\mathrm{II}} &= \sqrt{k_0^2-\left(\frac{x_{m1}}{b}\right)^2} \\ Y_m^{\mathrm{I}} &= \frac{k_{zm}^{\mathrm{I}}}{\omega\mu_0} \\ Y_m^{\mathrm{II}} &= \frac{k_{zm}^{\mathrm{I}}}{\omega\mu_0} \end{aligned} \tag{8}$$

and $k_0=\omega\sqrt{\epsilon_0\mu_0}$. The normalization constants g_m^i are given in terms of the derivative of J_1 by

$$g_m^{\mathrm{I}} = \frac{1}{\sqrt{\int_0^a \rho\,d\rho\,J_1^2\left(\frac{x_{m1}}{a}\rho\right)}} = \frac{\sqrt{2}}{a|J_1'(x_{m1})|} \tag{9}$$

$$g_m^{\mathrm{II}} = \frac{1}{\sqrt{\int_0^b \rho\,d\rho\,J_1^2\left(\frac{x_{m1}}{b}\rho\right)}} = \frac{\sqrt{2}}{b|J_1'(x_{m1})|} \tag{10}$$

and

$$\tilde{X}_i^{\mathrm{I}}(m) = g_m^{\mathrm{I}} \int_0^b X_i(\rho) J_1\left(\frac{x_{m1}}{a}\rho\right)\rho\, d\rho, \qquad i = 1, 2 \tag{11}$$

$$\tilde{X}_i^{\mathrm{II}}(m) = g_m^{\mathrm{II}} \int_0^b X_i(\rho) J_1\left(\frac{x_{m1}}{b}\rho\right)\rho\, d\rho, \qquad i = 1, 2. \tag{12}$$

To determine the functions X_1 and X_2, we expand them in series of basis functions

$$X_1(\rho) = \sum_{i=1}^{M} c_i^{\mathrm{I}} B_i(\rho)$$
$$X_2(\rho) = \sum_{i=1}^{M} c_i^{\mathrm{II}} B_i(\rho). \tag{13}$$

The same basis functions are used for both functions because the geometry is the same at the two discontinuity planes. Using the series expansions in the two integral equations and applying Galerkin's method, we get two sets of linear equations in the coefficients c_i^{I} and c_i^{II}. In matrix form, these can be written as

$$[A][c^{\mathrm{I}}] + [B][c^{\mathrm{II}}] = [U]$$
$$[B][c^{\mathrm{I}}] + [A][c^{\mathrm{II}}] = [0]. \tag{14}$$

The entries of the matrices $[A]$ and $[B]$ are given by

$$[A]_{ij} = \sum_{m=1}^{\infty} Y_m^{\mathrm{I}} \tilde{B}_i^{\mathrm{I}}(m)\tilde{B}_j^{\mathrm{I}}(m) + \sum_{m=1}^{\infty} Y_m^{\mathrm{II}} \frac{\tilde{B}_i^{\mathrm{II}}(m)\tilde{B}_i^{\mathrm{II}}(m)}{j\tan\left[k_{zm}^{\mathrm{II}} d\right]} \tag{15}$$

$$[B]_{ij} = -\sum_{m=1}^{\infty} Y_m^{\mathrm{II}} \frac{\tilde{B}_i^{\mathrm{II}}(m)\tilde{B}_i^{\mathrm{II}}(m)}{j\sin\left[k_{zm}^{\mathrm{II}} d\right]} \tag{16}$$

and

$$[U]_i = 2Y_1^{\mathrm{I}}\tilde{B}_i^{\mathrm{I}}(1). \tag{17}$$

Here, $[0]$ is a zero column vector. Once the expansion coefficients are determined, the reflected and transmitted waves are given by

$$S_{11} = -1 + \sum_{i=1}^{M} c_i^{\mathrm{I}} \tilde{B}_i^{\mathrm{I}}(1) \tag{18}$$

and

$$S_{21} = \sum_{i=1}^{M} c_i^{\mathrm{II}} \tilde{B}_i^{\mathrm{I}}(1). \tag{19}$$

For this type of filters, we examine two sets of basis functions, each of which includes the edge conditions. The first set is obtained by introducing a weighting function, which includes the proper singularity in combination with the modes of a circular waveguide, namely,

$$P_n(\rho) = \frac{J_1\left(\frac{x_{n1}}{b}\rho\right)}{\left(1-\left(\frac{\rho}{b}\right)^2\right)^{1/3}}, \qquad n = 1, 2, \ldots. \tag{20}$$

The second set is obtained from the local solutions of Maxwell's equations, as discussed in [14]. If we let r_n denote a zero of Bessel function of order $2/3$, the following set of basis functions are easily shown to satisfy the proper edge conditions:

$$Q_n(\rho) = J_{2/3}\left[r_n\left(1-\frac{\rho}{b}\right)\right], \qquad J_{2/3}(r_n) = 0,\ n = 1, 2, \ldots. \tag{21}$$

The integrals of the basis functions as given by (11) and (12) are evaluated numerically following procedures similar to those in [15].

III. Design of 1/8-Cut Dielectric-Ring Resonator Filters

Dielectric resonators are often used to reduce the size of microwave components. In the case under consideration, we focus attention on the design of microwave bandpass filters using 1/8-cut high-Q dielectric-ring resonators. The use of rings allows an increase in the Q factor as compared to rod resonators [7]. Furthermore, the location of the ring and its dimensions can be used to maximize the Q factor while achieving a substantial size reduction.

For simplicity, the coupling sections between the resonators consist of uniform sections of an empty below-cutoff 1/8-cut waveguide of the same radius as the loaded region. The length of the section is adjusted until the synthesis equations (1)–(4) are satisfied. If shorter coupling sections are desired, coupling irises can be used as in the iris-coupled TE_{01}-mode filter discussed above.

In order to determine the scattering parameters of the dominant slow mode at a coupling section, we need to know the normal modes of the dielectric-loaded region.

A. Modes of Dielectric Ring

We consider a dielectric ring of dielectric constant ϵ_2, as shown in Figs. 6 and 7. Mechanical support for the high dielectric ring is provided by a low dielectric material (ϵ_1) rod of radius R_1, the thickness of the dielectric ring is R_2–R_1 and the radius of the empty waveguide is R.

Since the incident mode TE_{01} has no angular dependence, it excites only TE_{0n} modes despite the presence of the dielectric. In particular, no complex modes are excited [16]. To determine the propagation constant β of the modes supported by the structure and the corresponding field distributions, we expand the axial component H_z in the three regions as follows [cf. Fig. 7(b)]:

$$H_z^{\mathrm{I}}(\rho) = AJ_0(k_1\rho)$$
$$k_1^2 + \beta^2 = k_0^2\epsilon_1 \tag{22}$$
$$H_z^{\mathrm{II}}(\rho) = BJ_0(k_2\rho) + CY_0(k_2\rho)$$
$$k_2^2 + \beta^2 = k_0^2\epsilon_2 \tag{23}$$

and

$$H_z^{\mathrm{III}}(\rho) = D\big(J_0(k_3\rho)Y_1(k_3R) - Y_0(k_3\rho)J_1(k_3R)\big)$$
$$k_3^2 + \beta^2 = k_0^2. \tag{24}$$

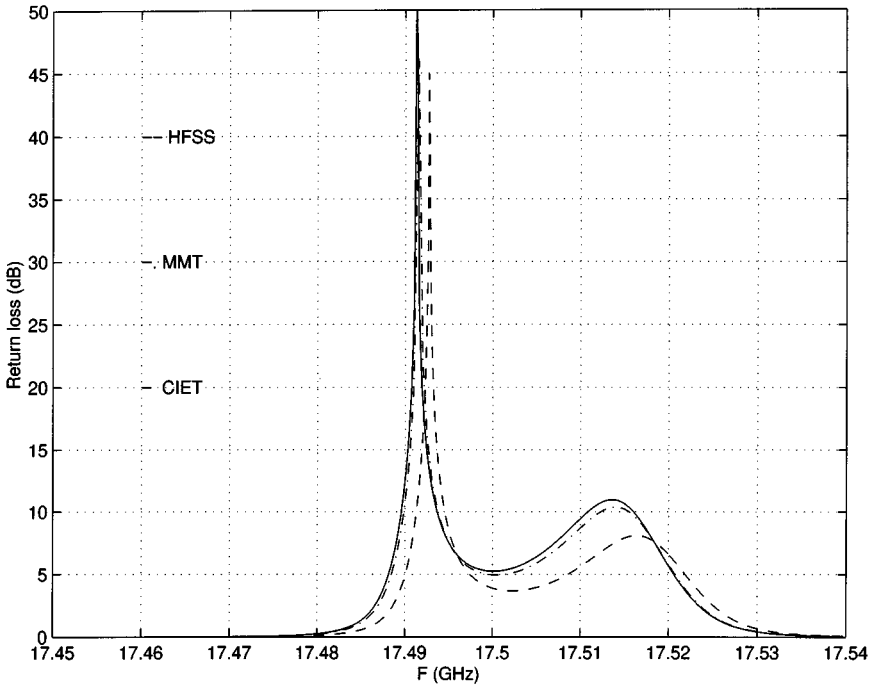

Fig. 2. Insertion loss of Filter I versus frequency. Solid line: CIET, dashed line: HFSS, dotted–dashed line: MMT. CIET and MMT results are identical.

By matching E_ϕ and H_z at the interfaces between the three regions, we obtain a transcendental equation for the propagation constant. This equation along with other relevant coupling integrals are given in the Appendix. The propagation constants of the propagating and evanescent modes are to be determined from this equation using any of the standard root-finding algorithms. Once the roots of the transcendental equation are located, the expansion coefficients A, B, C, and D are determined, thereby specifying the field distribution of the mode.

B. Scattering Parameters of Coupling Sections

The next step in the design of the filter consists in accurately determining the scattering parameters of the dominant slow mode at the coupling section, which consists of a portion of below-cutoff waveguide of length d (Fig. 7). The formulation is the same as in the case of the iris-coupled case discussed above, except for the expressions of the coupling integrals, which are now frequency dependent due to the presence of the dielectric-loaded regions.

From our numerical experiments, taking the modes of the dielectric-loaded region as basis functions is sufficient as long as the dielectric constant is not too large, less than, say, 100; most dielectric materials in use fall within this range.

It may be worth mentioning that the standard rules of thumb used to circumvent the phenomenon of relative convergence in the MMT fail in this case since the two regions, i.e., the dielectrically loaded and the empty 1/8-cut waveguide, have the same cross section. Within the CIET, the modes of the different regions appear only in computing the inner products and, therefore, the phenomenon of relative convergence is eliminated altogether. However, it is still not obvious which set of modes to use as basis functions within the CIET; those of the dielectric-loaded region or the empty one. The solution lies in examining the field distribution of the two sets. Since the modes of the dielectric-loaded region are more localized, or concentrated, in the high dielectric region over the cross section, a large number of modes in the empty region are needed to reproduce them. It is, therefore, more efficient to take the modes of the dielectric-loaded regions as basis functions.

With this choice of basis functions, the orthogonality of the modes can be fruitfully used to simplify the expressions of the entries of the matrices in (15) and (16).

Once all the coupling sections and lengths of the resonators are determined, the analysis of an assembled filter is carried out by using all basis functions at all discontinuities simultaneously. This procedure of the CIET is described in [2] and need not be repeated here.

IV. Numerical Results

A number of filters of varied characteristics were designed using the framework described here; illustrative cases are now presented.

To validate the approach and the programs, we first analyzed a TE_{01} filter, referred to as Filter I, whose dimensions were published in [17]. The filter consists of four irises of thickness $d = 0.2$ mm and inner radii $b_1 = b_4 = 3.888$ mm and $b_2 = b_3 = 6.718$ mm. The separations between the irises are $L_1 = L_3 = 10.907$ mm, $L_2 = 11.142$ mm, and the radius of the empty waveguide is $a = 16.269$ mm.

To our surprise, our CIET and MMT results, which are shown in Fig. 2, differ significantly from those in this reference (see [17, Fig. 8(a)]) where a minimum in-band return loss of 20 dB

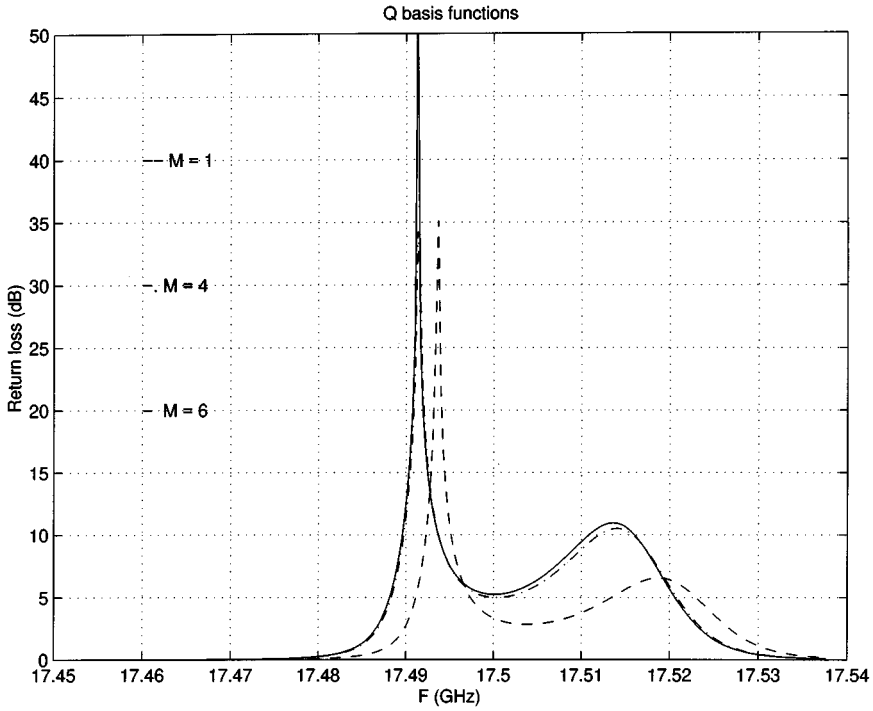

Fig. 3. Return loss of Filter I for $M = 1, 4$, and 6 Q basis functions.

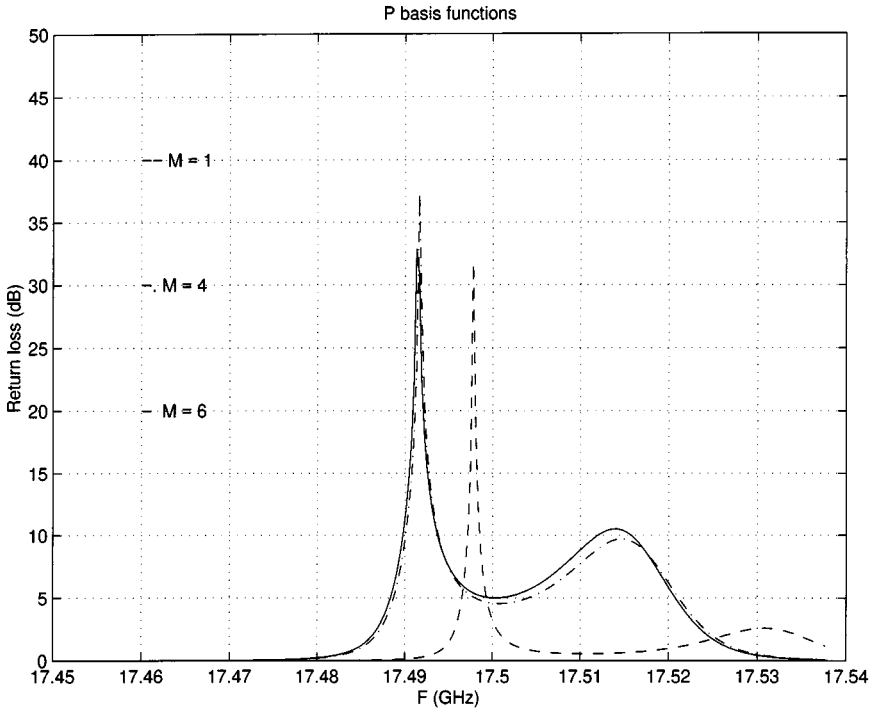

Fig. 4. Return loss of filter 1 for $M = 1, 4$, and 6 P basis functions.

is reported. The solid line is the CIET calculation with six basis functions and 100 terms in the sums involved in computing the matrix elements. The dashed–dotted line, which coincides with the solid line, is obtained from the MTT using 100 modes.

The filter was then simulated using the commercial software package HFSS; the obtained results, shown as the dashed line in Fig. 2, show good agreement with those obtained from the CIET and MMT. The slight difference between the results obtained from HFSS and the two other methods is attributed to the fact that, for this extremely narrow-band filter, HFSS memory requirement exceeds the 800 MB we have available.

The convergence of the CIET for the two sets of basis functions given by (20) and (21) was also investigated. Figs. 3 and 4 present the results obtained with the two different sets of basis functions. Both sets Q_n (Fig. 3) and P_n (Fig. 4) converge with about six basis functions when 100 modes are used to compute

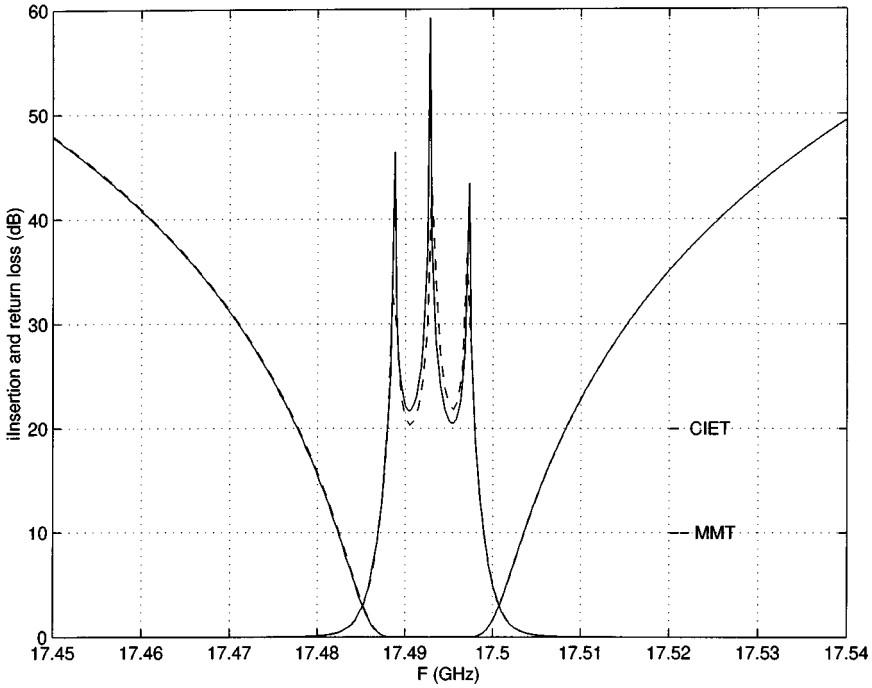

Fig. 5. Insertion and return loss of Filter II versus frequency. Solid line: CIET with ten basis functions, dashed line: MMT using 150 modes.

the entries of matrices. Obviously, the set Q_n in Fig. 3 shows slightly better convergence than the set P_n of Fig. 4. We attribute this to the fact that Q_n are derived from local solutions to Maxwell's equations. It is worth noting that the solid line in Fig. 3 (i.e., set Q_n with six basis functions) agrees with the solid line of Fig. 3 (regular mode matching with 100 modes) to within the plotting accuracy. The set P_n requires one more basis function (seven, Fig. 4) to achieve the same accuracy. The advantage of the set Q_n over P_n is even better, which is shown by the results obtained from only one basis function of each set (compare curves $M = 1$ in Figs. 3 and 4).

Having established the validity of the CIET programs, a filter with similar specifications was then designed using the approach described in this paper and analyzed using the CIET and MMT. This filter is referred to as Filter II. The thickness of the coupling irises is maintained at 0.2 mm, $2b_1 = 12.091$ mm, $2b_2 = 6.827$ mm, and the radius of the empty waveguide is 12.274 mm. The lengths of the three resonators are $l_1 = l_3 = 15.959$ mm and $l_2 = 16.297$ mm. Fig. 5 shows that all the original specifications are met and that the two methods yield comparable results. The design of the filter was carried out using ten basis functions and 150 terms in the sums; such a large number is required given the bandwidth of the filter. The dimensions given by the design program were rounded off to within 1 μm. The assembled filter was then analyzed using up to 20 basis functions and 200 terms in the sums.

To further test the approach, a fourth-order dielectric-resonator filter was designed and analyzed using both the CIET and HFSS. The desired minimum return loss in the passband extending from 2.2 to 2.3 GHz is 25 dB.

The cross section of the dielectric-loaded resonators has $R_1 = 38.675$ mm, $R_2 = 41.651$ mm, $R_0 = 59.501$ mm, $\epsilon_1 = 1.03$, and $\epsilon_2 = 23$.

To avoid the complications introduced by the feeding connections, which are eventually adjusted experimentally, we simply connected the first and last resonators to a long dielectric-loaded waveguide of the same cross section as the resonators. The filter is thus fed by the dominant slow mode corresponding to the resonant $\mathrm{TE}_{01\delta}$ of a resonator of finite length. The coupling gaps at the input and output are determined from the specifications of the filter. Actual feed networks can be designed using microstrip loops [4] or aperture-coupled rectangular waveguides [7].

Once the cross section of the resonators is fixed by maximizing its Q factor, i.e., the program determines the length of the five coupling sections as well as the four resonators as $d_1 = 13.762$ mm, $d_2 = 18.124$ mm, $d_3 = 35.201$ mm, $d_4 = 17.126$, and $d_5 = 41.842$ mm. The effect of the coupling on the resonant frequency of the resonators is thus fully taken into account. Typical filters designed along these lines were presented in [18].

The designed filter is shown in Figs. 6 and 7. Its insertion and return losses versus frequency are shown in Fig. 8. The solid line is obtained from a CIET analysis with eight basis functions and 80 terms in the sums. More basis functions were used and yielded negligible differences. The dashed line, obtained from HFSS, is in good agreement with the CIET calculations. The differences for small values of the reflection coefficient in the passband are attributed to the prescribed relative accuracy in the HFSS calculation, which was set to 0.4%. Higher accuracy would require finer discretization meshes and, consequently, more memory.

The error in the obtained center frequency from both methods, as determined from the analysis of the designed filter, is less than 0.1%, but the obtained bandwidth is about 0.5% larger than specified.

To illustrate the size reduction that can be achieved by using the dielectric resonators, we designed and analyzed a four-resonator iris-coupled 1/8-cut TE_{01}-mode filter with the same

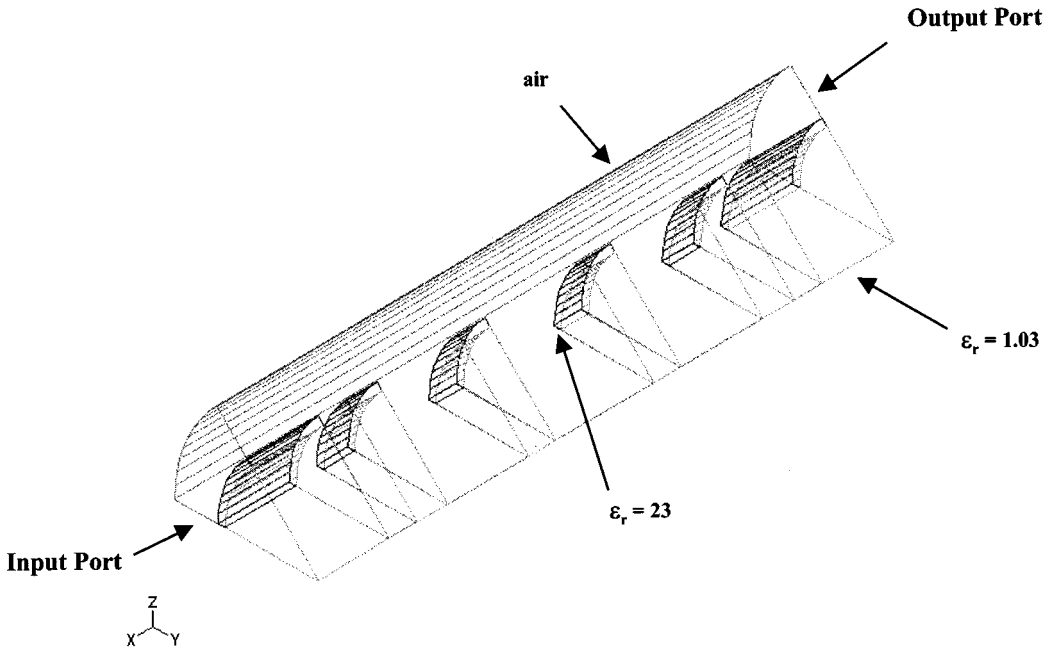

Fig. 6. Designed dielectric-resonator filter.

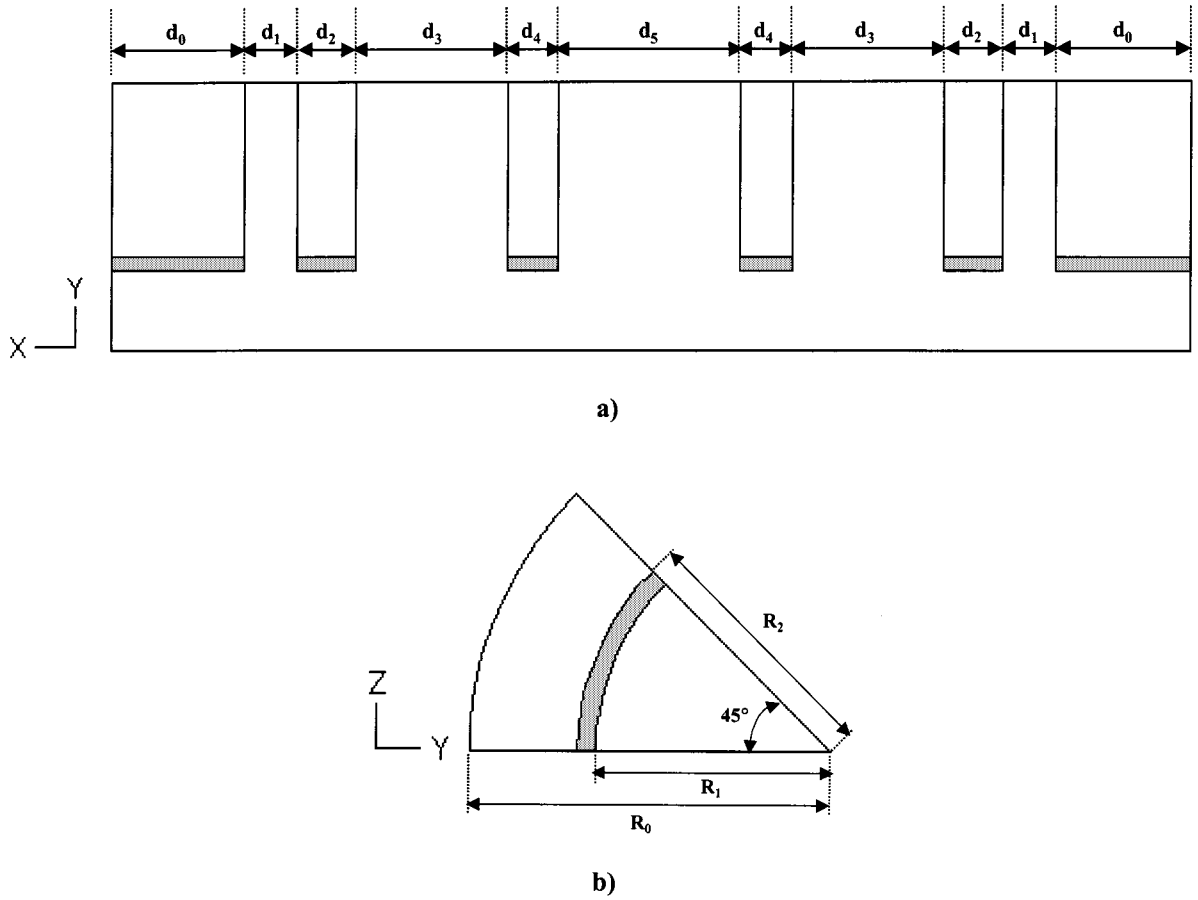

Fig. 7. (a) Side view and (b) cross section of designed dielectric-resonator filter.

specifications. Despite the small thickness of the coupling irises, the introduction of the dielectric resonators reduces the volume of the filter by a factor of about three. If the below-cutoff coupling sections in the dielectric-loaded filter were replaced by coupling irises of the same thickness as in the TE_{01}-mode filter, the volume would be reduced by a factor of nine instead of three;

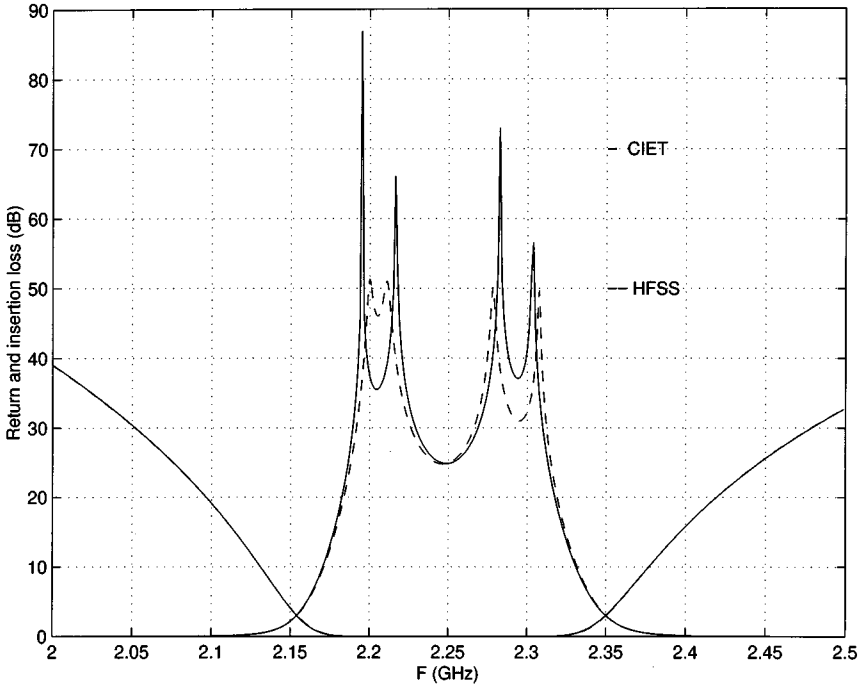

Fig. 8. Insertion and return loss (in decibels) of the designed dielectric-loaded resonator filter. Solid line: CIET using eight basis functions, dashed line: finite element (HFSS).

this ratio can be increased further by using dielectrics of higher dielectric constant. In this comparison, the volumes of the input and output dielectric sections are not included since they are not present in an actual implementation, as discussed above.

An attempt to accurately determine the effect of metallic losses on the performance of the filter using HFSS was made, but the amount of computer memory available on our computers is not sufficient for such a calculation. If we assume an unloaded Q of 2000, the in-band insertion loss can be estimated to be of the order of 0.7 dB for this filter [11].

V. Conclusions

Microwave bandpass filters using 1/8-cut circular waveguides are designed and accurately analyzed using globalized local solutions of Maxwell's equations in the CIET. Direct-coupled 1/8-cut dielectric-resonator filters using high-Q dielectric rings are also designed and analyzed using the same approach. Effects of the coupling sections on the resonant frequencies of the resonators are systematically included in the design. Numerical results using the CIET agree well with those of the standard MMT and the commercial software package HFSS.

Appendix

Here, the transcendental equation for the propagation constant β of a dielectric ring, as well as some coupling integrals, which we could not find in standard tables are presented. Only modes with no angular dependence are considered. The separation constants k_1, k_2, and k_3 are related to β by (10)–(13), J and Y are Bessel and Neumann functions

$$a_{11}a_{22} - a_{12}a_{21} = 0$$

where

$$\begin{aligned}
a_{11} =& k_1 J_0(k_1R_1)J_1(k_2R_1) - k_2 J_0(k_2R_1)J_1(k_1R_1)\\
a_{12} =& k_1 J_0(k_1R_1)Y_1(k_2R_1) - k_2 J_1(k_1R_1)Y_0(k_2R_1)\\
a_{21} =& k_2 J_0(k_2R_2)\big[J_1(k_3R_2)Y_1(k_3R) - J_1(k_3R)Y_1(k_3R_2)\big]\\
& - k_3 J_1(k_2R_2)\big[J_0(k_3R_2)Y_1(k_3R) - J_1(k_3R)Y_0(k_3R_2)\big]\\
a_{22} =& k_2 Y_0(k_2R_2)\big[J_1(k_3R_2)Y_1(k_3R) - J_1(k_3R)Y_1(k_3R_2)\big]\\
& - k_3 Y_1(k_2R_2)\big[J_0(k_3R_2)Y_1(k_3R) - J_1(k_3R)Y_0(k_3R_2)\big].
\end{aligned}$$

To avoid complex arithmetic, which would otherwise result when k_1 or k_3 are imaginary, it is preferable to use modified Bessel functions I_0, I_0, K_0, K_1 directly in the field expansions and treat the different cases separately. The normalization of the modes in the dielectric-loaded region involves integrals of products of combinations of Bessel and Neumann functions. Most of these integrals are given in [19], those not listed there are as follows:

$$\begin{aligned}
&\int xI_1(ax)K_1(ax)\,dx\\
&\quad = \frac{1}{2a}\Big[x\big(I_0(ax)K_1(ax) - I_1(ax)K_0(ax)\big)\\
&\qquad + ax^2\big(I_1(ax)K_1(ax) - I_0(ax)K_0(ax)\big)\Big]\\
&\int xJ_1(ax)Y_1(ax)\,dx\\
&\quad = -\frac{1}{2a}\Big[x\big(J_0(ax)Y_1(ax) + J_1(ax)Y_0(ax)\big)\\
&\qquad - ax^2\big(J_1(ax)Y_1(ax) + J_0(ax)Y_0(ax)\big)\Big].
\end{aligned}$$

REFERENCES

[1] T. Itoh, Ed., *Numerical Techniques for Microwave and Millimeter-Wave Passive Structures*. New York: Wiley, 1989.

[2] S. Amari, J. Bornemann, and R. Vahldieck, "Fast and accurate analysis of waveguide filters by the coupled-integral-equation technique," *IEEE Trans. Microwave Theory Tech.*, vol. 45, pp. 1611–1618, Sept. 1997.

[3] J. Bornemann, U. Rosenberg, S. Amari, and R. Vahldieck, "Edge-conditioned vector basis functions for the analysis and optimization of rectangular waveguide dual-mode filters," in *IEEE MTT-S Int. Microwave Symp. Dig.*, Anaheim, CA, June 1999, pp. 1695–1698.

[4] W. H. Harrison, "A miniature high-Q bandpass filter employing dielectric resonators," *IEEE Trans. Microwave Theory Tech.*, vol. MTT-16, pp. 210–218, Apr. 1968.

[5] S. B. Cohn, "Microwave bandpass filters containing high-Q dielectric resonators," *IEEE Trans. Microwave Theory Tech.*, vol. MTT-16, pp. 218–227, Apr. 1968.

[6] T. Hishikawa, K. Wakino, K. Tsunoda, and Y. Ishikawa, "Dielectric high-power bandpass filter using quarter-cut $TE_{01\delta}$ image resonator for cellular base stations," *IEEE Trans. Microwave Theory Tech.*, vol. MTT-35, pp. 1150–1155, Dec. 1987.

[7] Y. Kobayashi and M. Minegishi, "Precise design of a bandpass filter using high-Q dielectric ring resonators," *IEEE Trans. Microwave Theory Tech.*, vol. MTT-35, pp. 1156–1160, Dec. 1987.

[8] K. A. Zaki and C. Chen, "Coupling of nonaxially symmetric hybrid modes in dielectric resonators," *IEEE Trans. Microwave Theory Tech.*, vol. MTT-35, pp. 1136–1142, Dec. 1987.

[9] H. Kubo, H. Yamashita, and I. Awai, "Analysis of dielectric E-plane waveguides and design of filters," *IEEE Trans. Microwave Theory Tech.*, vol. 46, pp. 1085–1090, Aug. 1998.

[10] A. Abdelmonem, J. Liang, H. Yao, and K. A. Zaki, "Full-wave design of spurious free DR TE mode bandpass filters," *IEEE Trans. Microwave Theory Tech.*, vol. 43, pp. 744–752, Apr. 1995.

[11] G. L. Matthaei, L. Young, and E. M. T. Jones, *Microwave Filters, Impedance Matching Networks and Coupling Structures*. New York: McGraw-Hill, 1964.

[12] S. B. Cohn, "Theory of direct-coupled cavity filters," *Proc. IRE*, vol. 45, pp. 187–196, Feb. 1957.

[13] R. Levy, "Theory of direct-coupled-cavity filters," *IEEE Trans. Microwave Theory Tech.*, vol. MTT-15, pp. 340–348, June 1967.

[14] S. Amari, A. Motamedi, J. Bornemann, and R. Vahldieck, "Global edge-conditioned basis functions from local solutions of Maxwell's equations," in *IEEE MTT-S Int. Microwave Symp. Dig.*, Denver, CO, June 1997, pp. 1373–1376.

[15] S. Amari and J. Bornemann, "Efficient numerical computation of singular integrals with applications to electromagnetics," *IEEE Trans. Antennas Propagat.*, vol. 43, pp. 1343–1348, Nov. 1995.

[16] A. S. Omar and K. F. Schünemann, "Complex and backward-wave modes in inhomogeneously and anisotropically filled waveguides," *IEEE Trans. Microwave Theory Tech.*, vol. MTT-35, pp. 268–275, Mar. 1987.

[17] U. Papziner and F. Arndt, "Field theoretical computer-aided design of rectangular and circular iris coupled rectangular and circular waveguide cavity filters," *IEEE Trans. Microwave Theory Tech.*, vol. 41, pp. 462–471, Mar. 1993.

[18] S. Amari, R. Vahldieck, and J. Bornemann, "Full-wave design and analysis of bandpass filters using 1/8-cut high-Q dielectric ring resonators," in *Proc. 28th European Microwave Conf.*, Amsterdam, The Netherlands, Oct. 1998, pp. 424–427.

[19] I. S. Gradshteyn and I. M. Ryznik, *Tables of Integrals, Series, and Products*, 2nd ed. New York: Academic, 1994.

Smain Amari (M'98) received the D.E.S. degree in physics and electronics from Constantine University, Constantine, Algeria, in 1985, and the M.S. degree in electrical engineering and Ph.D. degree in physics from Washington University, St. Louis, MO, in 1989 and 1994, respectively.

Since 1994, he has been with the Department of Electrical and Computer Engineering, University of Victoria, Victoria, BC, Canada. He is interested in numerical methods in electromagnetics, numerical analysis, applied mathematics, applied physics, and application of quantum-field theory in quantum many-particle systems.

Jens Bornemann (M'97–SM'90) received the Dipl.-Ing. and Dr.-Ing. degrees from the University of Bremen, Bremen, Germany, in 1980 and 1984, respectively, both in electrical engineering.

From 1984 to 1985, he was a Consulting Engineer. In 1985, he joined the University of Bremen, as an Assistant Professor. Since April 1988, he has been with the Department of Electrical and Computer Engineering, University of Victoria, Victoria, BC, Canada, where he became a Professor in 1992. From 1992 to 1995, he was a Fellow of the British Columbia Advanced Systems Institute. In 1996, he was a Visiting Scientist at Spar Aerospace, Montreal, QC, Canada, and a Visiting Professor in the Microwave Department, University of Ulm, Ulm, Germany. Since 1997, he has been a Co-Director of the Center for Advanced Materials and Related Technology (CAMTEC), University of Victoria. He co-authored *Waveguide Components for Antenna Feed Systems. Theory and CAD* (Norwood, MA: Artech House, 1993) and has authored/co-authored over 160 technical papers. His research activities include microwave/millimeter-wave components and systems design, and problems involving electromagnetic-field theory in integrated circuits, waveguide feed networks, and radiating structures. He serves on the Editorial Advisory Board of the *International Journal of Numerical Modeling*.

Dr. Bornemann is a Registered Professional Engineer in the Province of British Columbia. He is a senior member of the IEEE Microwave Theory and Techniques and IEEE Antennas and Propagation Societies. He currently serves as an Associate Editor for the IEEE TRANSACTIONS ON MICROWAVE THEORY AND TECHNIQUES in the area of microwave modeling and computer-aided design (CAD). He was a recipient of the 1983 A. F. Bulgin Premium presented by the Institution of Electronic and Radio Engineers.

Alexandre Laisné was born in Villedieu-les-Poeles, France, in 1976. He received the Engineering Diploma in electrical engineering from the National Institute of Applied Sciences (INSA), Rennes, France, in 1999, the Masters degree in electronics and electrical engineering (with distinction) from Strathclyde University, Glasgow, Scotland, in 1999, and is currently working toward the Ph.D. degree at the INSA.

During the summer of 1999, he was with he Optical Computing Laboratory, Colorado State University, Boulder, where he was involved with research on holographic memories. During the summer of 1999, he joined the CADMIC Group, University of Victoria, Victoria, BC, Canada, where his research was based on simulation of filters with HFSS. He is currently involved with the simulation of dielectric-resonator antennas with finite difference time domain (FDTD) in the Laboratory of Components and Telecommunications Systems, INSA.

Rüdiger Vahldieck (M'85–SM'86–F'99) received the Dipl.-Ing. and Dr.-Ing. degrees in electrical engineering from the University of Bremen, Bremen, Germany, in 1980 and 1983, respectively.

From 1984 to 1986, he was a Research Associate at the University of Ottawa. In 1986, he joined the Department of Electrical and Computer Engineering, University of Victoria, Victoria, BC, Canada, where he became a Full Professor in 1991. During Fall and Spring of 1992–1993, he was a Visiting Scientist at the Ferdinand-Braun-Institute für Hochfrequenztechnik, Berlin, Germany. Since 1997, he has been a Professor of field theory at the Swiss Federal Institute of Technology, Zürich, Switzerland. He has authored or co-authored over 170 technical papers in books, journals, and conferences, mainly in the field of microwave CAD. His research interests include numerical methods to model electromagnetic fields in the general area of electromagnetic compatibility (EMC) and, in particular, for CAD of microwave, millimeter-wave, and opto-electronic integrated circuits.

Prof. Vahldieck was the president of the IEEE 2000 International Zürich Seminar on Broadband Communications (IZS'2000) and vice president of the EMC Congress, Zürich, Switzerland. He is a member of the Editorial Board of the IEEE TRANSACTIONS ON MICROWAVE THEORY AND TECHNIQUES. Since 1992, he has also served on the Technical Program Committee of the IEEE International Microwave Symposium, the IEEE Microwave Theory and Techniques Society (IEEE MTT-S) Technical Committee on Microwave Field Theory and, in 1999, on the Technical Program Committee of the European Microwave Conference. He is the chairman of the IEEE Swiss Joint Chapter of the IEEE MTT-S, IEEE Antennas and Propagation Society (IEEE AP-S), and IEEE Electromagnetic Compatibility Society (IEEE EMC-S). Together with three co-authors, he received the 1995 J. K. Mitra Award of the Institution of Electronics and Telecommunication Engineers (IETE) for the Best Research Paper.